Development/Plasticity/Repair

The Neurosteroid Allopregnanolone Promotes Proliferation of Rodent and Human Neural Progenitor Cells and Regulates Cell-Cycle Gene and Protein Expression

Jun Ming Wang,[1] Patrick B. Johnston,[2] Bret Gene Ball,[3] and Roberta Diaz Brinton[1]

[1]Department of Molecular Pharmacology and Toxicology and Program in Neuroscience, Pharmaceutical Science Center, University of Southern California, Los Angeles, California 90033, [2]Division of Hematology, Department of Internal Medicine, Mayo Clinic, Rochester, Minnesota 55905, and [3]Gene Therapy Laboratories, Department of Biochemistry, Keck School of Medicine, University of Southern California, Los Angeles, California 90033

Our previous research demonstrated that the neuroactive progesterone metabolite allopregnanolone (3α-hydroxy-5α-pregnan-20-one) rapidly induced hippocampal neuron neurite regression (Brinton, 1994). We hypothesized that allopregnanolone-induced neurite regression was a prelude to mitogenesis initiated by a rise in intracellular calcium. Supporting this hypothesis, the current data demonstrate that allopregnanolone, in a dose-dependent manner, induces a significant increase in proliferation of neuroprogenitor cells (NPCs) derived from the rat hippocampus and human neural stem cells (hNSCs) derived from the cerebral cortex. Proliferation was determined by incorporation of bromodeoxyuridine and [^{3}H]thymidine, fluorescence-activated cell sorter analysis of murine leukemia virus–green fluorescent protein-labeled mitotic NPCs, and total cell number counting. Allopregnanolone-induced proliferation was isomer and steroid specific, in that the stereoisomer 3β-hydroxy-5β-pregnan-20-one and related steroids did not increase [^{3}H]thymidine uptake. Immunofluorescent analyses for the NPC markers nestin and Tuj1 indicated that newly formed cells were of neuronal lineage. Furthermore, microarray analysis of cell-cycle genes and real-time reverse transcription-PCR and Western blot validation revealed that allopregnanolone increased the expression of genes that promote mitosis and inhibited the expression of genes that repress cell proliferation. Allopregnanolone-induced proliferation was antagonized by the voltage-gated L-type calcium channel (VGLCC) blocker nifedipine, consistent with the finding that allopregnanolone induces a rapid increase in intracellular calcium in hippocampal neurons via a GABA type A receptor-activated VGLCC (Son et al., 2002). These data demonstrate that allopregnanolone significantly increased rat NPC and hNSC proliferation with concomitant regulation in mitotic cell-cycle genes via a VGLCC mechanism. The therapeutic potential of allopregnanolone as a neurogenic molecule is discussed.

Key words: **allopregnanolone; neurogenesis; hippocampus; cell-cycle genes; L-type calcium channel; therapeutics**

Introduction

The neurosteroid allopregnanolone (APα) (3α-hydroxy-5α-pregnan-20-one) is a reduced metabolite of progesterone (P_4) and is generated *de novo* in the CNS (for review, see Melcangi et al., 1999; Baulieu et al., 2001; Mellon and Griffin, 2002b). Developmentally, P_4 and APα are synthesized in the CNS throughout the embryonic period in the pluripotential progenitor cells (Lauber and Lichtensteiger, 1996; Gago et al., 2004) and reach their highest concentration in late gestation (Pomata et al., 2000; Grobin and Morrow, 2001). In the aged and Alzheimer's disease (AD) brain, both the pool of neural stem cells (NSCs) and their proliferative potential are markedly diminished (Bernardi et al., 1998; Genazzani et al., 1998). In parallel, APα content is diminished in the brains of AD patients compared with age-matched controls (Weill-Engerer et al., 2002).

Functional analyses indicate that APα induces myelin formation in both the CNS and the peripheral nervous system (Baulieu and Schumacher, 2000; Schumacher et al., 2003) and promotes neuron survival in the presence of excitotoxic insults (Brinton, 1994; Ciriza et al., 2004). Griffin et al. (2004) recently reported that APα can delay the onset and severity of neurodegenerative pathology in a mouse model of Niemann-Pick's disease.

In mature neurons, APα is well known as an allosteric modulator of the $GABA_A$ receptor ($GABA_AR$)/chloride channel to increase chloride influx, thereby hyperpolarizing the neuronal membrane potential and decreasing neuron excitability (Gee et al., 1992; Brinton, 1994; Grobin and Morrow, 2001; Liu et al., 2002). These properties led to the pursuit of APα and derivatives as an antiepileptic and antianxiety therapeutic drug (Monaghan et al., 1997; Kerrigan et al., 2000). In marked contrast, the flux of chloride in developing neurons is opposite to that of mature neurons (Cherubini et al., 1990; Perrot-Sinal et al., 2003). In immature neurons, the high intracellular chloride content leads to an efflux of chloride through the $GABA_AR$ depolarization of

Received Nov. 3, 2004; revised March 23, 2005; accepted March 26, 2005.

This research was supported by grants from the Kenneth T. and Eileen L. Norris Foundation and the L. K. Whittier Foundation (R.D.B.). We thank Dr. Clive Svendsen for the gift of human neural stem cells (Mo27Cx, P3).

Correspondence should be addressed to Dr. Roberta D. Brinton, Department of Molecular Pharmacology and Toxicology, Pharmaceutical Sciences Center, University of Southern California, 1985 Zonal Avenue, Los Angeles, CA 90089-9121. E-mail: rbrinton@hsc.usc.edu.

DOI:10.1523/JNEUROSCI.4520-04.2005

 0270-6474/05/254706-13$15.00/0

the membrane and opening of L-type voltage-gated Ca^{2+} channels (VGLCCs) (Dayanithi and Tapia-Arancibia, 1996; Son et al., 2002; Ben-Ari et al., 2004; van den Pol, 2004). Thus, the $GABA_AR$-mediated depolarization could be a trigger for a spontaneous, activity-independent $[Ca^{2+}]_i$ rise in early precursor cells or subventricular zone radial precursor cells, thereby influencing developmental events, such as neurogenesis and synaptogenesis (Owens et al., 2000; Ashworth and Bolsover, 2002; Deisseroth et al., 2004).

Previous work from our laboratory demonstrated that exposure of embryonic day 18 (E18) rat hippocampal neurons to APα induced regression of neurite outgrowth within 1 h (Brinton, 1994). Subsequent microscopic morphological observation indicated that APα significantly increased the number of cells exhibiting morphological features of mitotic events (our unpublished observations). These findings led us to hypothesize that APα promoted hippocampal progenitor cell proliferation to thereby act as a neurogenic agent. Therefore, we undertook a series of cellular, morphological, biochemical, and genomic analyses to determine the neurogenic potential of APα in cultured rat neural progenitor cells (rNPCs) and human NSCs (hNSCs).

Materials and Methods

Animals. Timed-pregnant Sprague Dawley rats were purchased from Harlan Sprague Dawley (Indianapolis, IN). These rats were housed at 24°C on a 14/10 h light/dark cycle, fed with regular rat chow, and allowed tap water *ad libitum*. All studies were approved by the University of Southern California Institutional Review Board for animal care.

Steroids. All steroids used in this study were purchased from Steraloids (Newport, RI). They are as follows: APα, epipregnanolone (APβ) (5β-pregnan-3β-ol-20-one), epiallopregnanolone (5α-pregnan-3β-ol-20-one), P_4, allopregnanediol (5α-pregnan-3α, 20α-diol), allopregnanetriol (5α-pregnan-3α, 17, 20α-triol), 5α-pregnan-3β-ol, and pregnenolone sulfate (5-pregnan-3β-ol-20-one sulfate).

Hippocampal neuronal culture. Primary cultures of dissociated hippocampal neurons were performed as described previously (Nilsen and Brinton, 2003). Briefly, hippocampi were dissected from the brains of E18 rat fetuses, treated with 0.02% trypsin in HBSS (Invitrogen, Grand Island, NY) for 5 min at 37°C, and dissociated by repeated passage through a series of fire-polished constricted Pasteur pipettes. Cells were plated on poly-D-lysine-coated 60 mm Falcon Petri dishes at a density of $0.5–1 \times 10^5$ cells/cm^2 for biochemical study. Cells were plated on Nalge Nunc (Naperville, IL) CC2-coated four-well chamber slides at a density of $2–4 \times 10^4$ cells/cm^2 for morphological study or on laminin-coated cell culture-grade black clear-bottom 96-well Falcon plates at a density of $7.5–15 \times 10^4$ cells per well for 5-bromo-2-deoxyuridine (BrdU) incorporation chemiluminescence immunoassay. Nerve cells were grown in Neurobasal medium (Invitrogen, Carlsbad, CA) supplemented with 10 U/ml penicillin, 10 μg/ml streptomycin, 0.5 mM glutamine, 25 μM glutamate, and 2% B27 (Invitrogen, Gaithersburg, MD). Cultures were maintained at 37°C in a humidified 5% CO_2 atmosphere. All experiments were performed at the times indicated.

Culture of human neural stem cells. Human embryonic brain cortical stem cells (gift from Dr. Svendsen, Departments of Anatomy and Neurology and the Waisman Center, University of Wisconsin, Madison, WI) were provided as cryopreserved neurospheres. Neurospheres were cultured as described previously by Dr. Svendsen's laboratory (Wachs et al., 2003) in DMEM/Ham's F-12 medium (7:3) containing penicillin/streptomycin/amphotericin B (1%), supplemented with B27 (2%; Invitrogen, Gaithersburg, MD), epidermal growth factor (EGF) (20 ng/ml; Invitrogen, Gaithersburg, MD), FGF-2 (20 ng/ml; Invitrogen, Gaithersburg, MD), and heparin (5 μg/ml; Sigma, St. Louis, MO) in a humidified incubator (37°C and 5% CO_2), and one-half of the growth medium was replenished every 3–4 d. Neurospheres were then mechanically triturated into single cells with flame-polished Pasteur pipettes, plated onto T75 flasks at a density equivalent to 2×10^6 cells per flask, and passaged every 14 d. After the second passage, cells were switched to maintenance media [DMEM/Ham's F-12 (7:3)] containing N_2 supplement (1%; Invitrogen), 20 ng/ml EGF, and 10 ng/ml LIF (Chemicon, Temecula, CA) and seeded onto T75 flasks coated with laminin (MP Biomedicals, Irvine, CA) at a density of 2×10^6 cells per flask, which were then plated onto laminin-coated 96-well plates at a density of $7.5–15 \times 10^4$ cells per well or chamber slides at a density of $2–4 \times 10^4$ cells/cm^2 before analysis.

Immunocytochemical staining. Immunocytochemistry was performed to check the cell composition in the culture and determine the cell lineage of the newly formed neurons. Hippocampal neurons, plated onto four-well chamber slides and allowed to seed for 1 h, were treated with 250 nM APα or vehicle for times as indicated in Results and fixed with 4% paraformaldehyde. Neurons were then incubated overnight with the following primary antibodies (Doetsch et al., 1997; Romero-Ramos et al., 2002): monoclonal antibody for neuronal class III β-tubulin [Tuj1; 1:500 (NPC marker); Covance, Berkeley, CA], monoclonal antibody for nestin [1:5000 (NSC marker); Chemicon], monoclonal antibody for myelin basic protein (MBP) [1:50 (oligodendrocyte marker); Research Diagnostics, Flanders, NJ], polyclonal antibody for glial fibrillary acidic protein (GFAP) [1:1000 (astrocyte marker); Santa Cruz Biotechnology, Santa Cruz, CA], and monoclonal antibody for microtubule-associated protein 2 (MAP2) [1:200 (neuronal cell marker); Sigma] for colabeling with GFAP or polyclonal antibody for MAP2 (1:1000; Chemicon) for colabeling with other mice-derived antibodies. After PBS wash, cells were incubated for 30 min in a mixture of secondary antibodies containing anti-mouse IgG or anti-rabbit IgG conjugated with FITC (1: 200; Vector Laboratories, Burlingame, CA) and anti-rabbit IgG or anti-mouse IgG conjugated with Texas Red (1:50; Vector Laboratories) according to the requirements of the first antibody and colabeling combination. Slides were washed three times for 10 min each with PBS, rinsed with water, and mounted under coverslips with 4′,6′-diamidino-2-phenylindole (DAPI)-containing mounting medium (Vector Laboratories). Labeled cells were observed by Zeiss (Oberkochen, Germany) Axiovert 200M fluorescent microscope, and images were captured by SlideBook software (Intelligent Imaging Innovations, San Diego, CA).

Human neuronal stem cells were plated into four-well chamber slides coated with laminin. The cells were immunostained for the neuronal stem cells markers nestin and Tuj1 as described above.

BrdU incorporation. Cell proliferation was first evaluated by measuring the incorporation of BrdU in the S phase of the cell cycle. BrdU incorporation was detected by using kits purchased from Roche (Penzberg, Germany). For immunofluorescent assay, cells were loaded with 10 μM BrdU after 1 h of seeding on chamber slides in the presence or absence of 250 nM APα and cultured for 1 d. After fixation with 4% paraformaldehyde, cells were then incubated with anti-BrdU working solution, a 1:10 dilution of antibody to incubation buffer (in mM: 66 Tris, pH 8.0, 0.66 $MgCl_2$, and 1 2-mercaptoethanol), for 30 min at 37°C. Cells were then incubated with anti-mouse IgG conjugated with fluorescein (1:10 in incubation buffer) for 30 min at 37°C. Chamber slides were mounted, cells were observed, and the images were captured as described above. For chemiluminescence immunoassay, rat hippocampal cells, after 1 h of seeding, were loaded with 10 μM BrdU in the presence or absence of mouse EGF (20 ng/ml) and 100 pM to 1000 μM APα in Neurobasal medium with B27 for 1 d, and human cerebral cortical stem cells, after overnight adhesion and then 4–5 h of starvation (medium without supplements), were loaded with 10 μM BrdU in the presence or absence of basic FGF (bFGF) and a different concentration of APα in complete maintenance medium for 1 d. The cells were then fixed using the Fixdenat solution (Roche) for 30 min, incubated with anti-BrdU peroxidase for 90 min, and further developed with substrate solution for 3 min. The plates were then read with an Lmax microplate luminometer (Molecular Devices, Sunnyvale, CA). After subtracting the value of the blank (without BrdU loading), the results were analyzed using a one-way ANOVA, followed by a Neuman–Keuls *post hoc* test, and presented as percentage increase versus control.

[^{3}H]thymidine uptake. The specificity of APα and its stereoisomers, as well as its parental neurosteroid progesterone, on DNA replication was determined by [^{3}H]thymidine uptake. Briefly, hippocampal neurons (1×10^5 per well) were seeded in poly-D-lysine-coated 24-well Falcon plates. After 1 h, neurons were loaded with 1 μCi/ml [^{3}H]thymidine in the presence or absence of 250 nM APα or its relative stereoisomers for

24 h. Neurons were washed three times with PBS to remove free [^{3}H]thymidine and collected by a rubber policeman. Cell lysates were counted in a Beckman counter (LS1801; Beckman Coulter, Fullerton, CA). Data are presented as mean ± SEM of three independent experiments conducted in triplicate.

Murine leukemia virus–enhanced green fluorescent protein viral particle preparation and cell labeling. To verify that APα-induced DNA amplification was indicative of mitosis and not DNA repair and that APα led to a complete mitosis, fluorescence-activated cell sorting (FACS) assay was performed to quantitatively measure the number of retrovirus–enhanced green fluorescent protein (eGFP)-labeled dividing rNPCs (Palmer et al., 1997; van Praag et al., 2002). The murine leukemia virus (MuLV)–GFP retrovirus integrates into the host genome only if nuclear envelope breakdown occurs, which takes place during mitosis and hence does not occur under conditions of DNA repair during which BrdU can also be incorporated. More importantly, MuLV is unable to infect growth-arrested cells or cells progressing through a partial cell cycle that includes S phase but not mitosis (Roe et al., 1993; Lewis and Emerman, 1994; Bieniasz et al., 1995). Thus, the GFP signal can only be observed in the cells that have transversed a complete cell cycle. Importantly, MuLV is unable to infect growth-arrested cells or cells progressing through a partial cell cycle that includes the S phase but not mitosis (Roe et al., 1993; Lewis and Emerman, 1994; Bieniasz et al., 1995). Therefore, an increase in the number of GFP-positive cells serves not only as a marker for proliferation but also as an indicator for complete mitosis.

Retroviral vector particles were produced by a three-plasmid expression system (Soneoka et al., 1995). In brief, 24 h before transfection, human embryonic kidney 293T (HEK293T) cells were split one to five and transferred to a 10 cm tissue culture plate. To transfect, 10 μg of retroviral vector containing *GFP* gene, which was constructed into a *PGK-eGFP* gene cassette between MuLV 5′ long-term repeat (LTR) plus a packaging signal and 3′ LTR (W. F. Anderson, University of Southern California, Los Angeles, CA); 10 μg of pCGP plasmid containing the viral *gag pol* genes, which encode the viral matrix, capsid, nucleoproteins, and reverse transcriptase (W. F. Anderson); and 10 μg of pCEE+ plasmid expressing the MuLV ecotropic envelope protein (MacKrell et al., 1996) were coprecipitated by calcium phosphate. The precipitate was added drop-wise to HEK293T cells at ~75% confluence. Twelve to 16 h after transfection, cells were washed with PBS warmed to 37°C, and then fresh medium was added. Thirty-six hours after transfection, viral supernatants were harvested and passed through a 0.45 μm filter (Millipore, Bedford, MA) to remove transfected cells and cellular debris. Final virus titers (labeled MuLV–eGFP) were 5–7 × 10^6 colony-forming units per milliliter as determined by FACS (Coulter Epics-XL Fluorescence-Activated Cell Sorter) analysis of transduced HEK293T controls.

Rat hippocampal neurons were seeded onto 60 mm Petri dishes for FACS analysis or slide chambers for fluorescent microscopy observation and were infected with MuLV–eGFP viral particles (2.5–3.5 × 10^6/ml) in the presence or absence of 500 nM APα, 500 nM APβ, 10 μM nifedipine, or nifedipine plus APα 1 h after seeding. After 4 h, cells were washed and further incubated with fresh media with steroids to allow for the GFP expression in infected cells.

HT-22 cell culture and MuLV–GFP infection. The immortalized mouse hippocampal HT-22 cell line (Sagara et al., 2002; Mize et al., 2003) was used as a positive control for labeling dividing cells by MuLV–GFP. Cells were cultivated in DMEM (high glucose, with L-glutamine, with pyridoxine hydrochloride; Invitrogen, Grand Island, NY) supplemented with 100 U/ml penicillin, 100 mg/ml streptomycin, and 5% FBS (heat inactivated). The cells were split 1–10 every 4 d. One day after splitting, the cells were infected with MuLV–GFP viral particles in the presence or absence of APα as described above.

FACS analysis and morphological observation of MuLV–GFP-positive cells. After 48 h of incubation, cells were trypsinized, suspended gently by pipetting up and down, and collected into a Falcon 12 × 75 mm tube (polystyrene). After fixation with 4% paraformaldehyde, the cells were then subjected to FACS analysis. In each sample, 2000 cells were sorted by Coulter Epics-XL Fluorescence Activated Cell Sorter, and the numbers of GFP-positive cells were given. The mouse hippocampal derived cell line HT-22 was used as a positive control, whereas primary 7 d *in vitro* (DIV) hippocampal neurons, which were without detectable mitotic activity as measured by BrdU labeling, were used as a negative control. The neuronal morphology of the GFP-positive cells was assessed using cells seeded on chamber slides. In addition, cells were immunostained with the NPC cell marker Tuj1 as described above.

Gene-array assay. To analyze cell-cycle gene regulation, a commercially available targeted cDNA array of 96 cell-cycle regulatory genes and two housekeeping genes (Cell Cycle GEArray Q series, version 1; SuperArray, Bethesda, MD) were used according to the instructions of the manufacturer. Briefly, primary cultures were treated with or without 500 nM APα for 24 h, and total RNA was isolated using TRIzol reagent (Invitrogen, Carlsbad, CA) as described by the manufacturer. Ten micrograms of total RNA were reverse transcribed into biotin-16-deoxy-UTP-labeled single-strand cDNA by Moloney murine leukemia virus reverse transcriptase. After prehybridization, membranes were hybridized with biotin-labeled cDNA probe and incubated with alkaline phosphatase-conjugated streptavidin. Chemiluminescence was visualized by autoradiography. The intensity of the spots was extracted using "ScanAlyze" software [developed by Michael Eisen at Lawrence Berkeley National Laboratory (Berkeley, CA), recommended by SuperArray]. The data were analyzed by GEArray Analyzer (SuperArray, version 1.3). β-Actin and glyceraldehyde-3-phosphate dehydrogenase (GAPDH) were used as internal controls. Bacterial plasmid (pUC18) was used as a negative control.

Real-time reverse transcription-PCR. Real-time reverse transcription (RT)-PCR was performed to validate the gene-array results. Total RNA was prepared as described above. cDNA was synthesized using SuperScript III reverse transcriptase (Invitrogen, Grand Island, NY) and oligo-dT primer in accordance with the protocols of the manufacturer. The expression of related genes was quantified using the SYBR green reagent (2× SYBR Green Supermix; Bio-Rad, Hercules, CA) following the instructions of the manufacturer on a Bio-Rad iCycler. PCR was performed in multiplicate in optimized conditions: 95°C denatured for 3 min, followed by 40 cycles of 45 s at 94°C, 45 s at 55°C, and 45 s at 72°C using the following primers: cyclin A2 (GenBank accession number XM_342229), forward, 5′-GCTTTTAGTGCCGCTGTCTC-3′, reverse, 5′-AGTGATGTCTGGCTGCCTCT-3′; cyclin B1 (GenBank accession number NM_171991), forward, 5′-CTGCTGCAGGAGACCATGTA-3′, reverse, 5′-CTACGGAGGAAGTGCAGAGG-3′; cyclin E (GenBank accession number D14015), forward, 5′-ATGTCCAAGTGGCCTACGTC-3′, reverse, 5′-TCTGCATCAACTCCAACGAG-3′; cell-dividing control protein 2 (CDC2) (GenBank accession number NM_019296), forward, 5′-CGGTTGACATCTGGAGCATA-3′, reverse, 5′-GCATTTTCGAGAGCAAGTCC-3′; proliferating cell nuclear antigen (PCNA) (GenBank accession number NM_022381), forward, 5′-TCACAAAAGCCACTCCACTG-3′, reverse, 5′-CATCTCAGAAGCGATCGTCA-3′; cyclin-dependent kinase inhibitor 2C (p18, inhibits CDK4) (Cdkn2c) (GenBank accession number NM_131902), forward, 5′-ACCGAACTGGTTTTGCTGTC-3′, reverse, 5′-GGGCAGGTTCCCTTCATTAT-3′; and ubiquitin-activating enzyme E1 (GenBank accession number XM_217252), forward, 5′-ACAATTGGCCCAGCTTAATG-3′, reverse, 5′-CTTGGAGTCAGTCAGCACCA-3′. No other products were amplified because melting curves showed only one peak in each primer pair. Fluorescence signals were measured over 40 PCR cycles. The cycle number (C_t) at which the signals crossed a threshold set within the logarithmic phase was recorded. For quantitation, we evaluated the difference in cycle threshold (ΔC_t) between the APα-treated group and vehicle control of each gene. The efficiency of amplification of each pair of primers was determined by serial dilutions of templates and all were >0.9. Each sample was normalized with the loading references β-actin and GAPDH. C_t values used were the means of triplicate replicates. Experiments were repeated at least three times.

Western blot analyses for CDC2 and PCNA protein expression. The effects of APα on gene expression were further validated at the protein level by Western blot analyses. APα was added to the cultures after a 1 h seeding period, and cells were lysed at the time points as indicated. Cells were washed with cold PBS and incubated in ice-cold lysis buffer consisting of 0.1% SDS, 1% Igepal CA-630 (nonionic, nondenaturing detergent), 0.2 mM phenylmethylsulfonylfluoride, and 0.01‰ protease inhib-

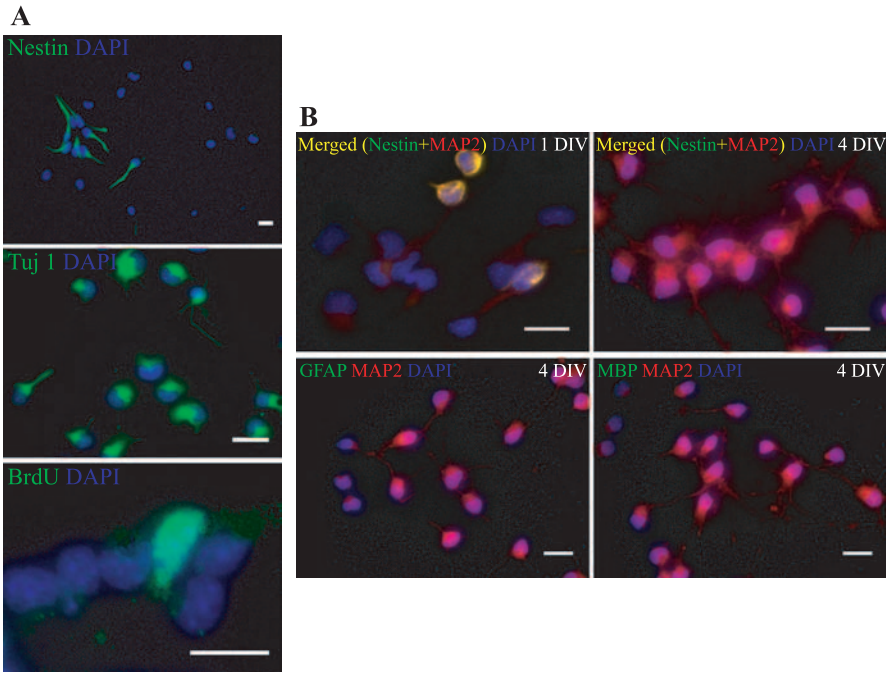

Figure 1. Characterization of neural progenitor cells in primary cultures of embryonic day 18 rat hippocampus. ***A***, At 1 DIV, nestin (top)-positive cells are clustered, and nestin immunoreactivity is apparent within the cytoplasmic compartment of both the cell body and neurites. Nonclustered cells are nestin negative. The middle shows that the majority of cells are Tuj1 positive. The bottom shows one cell with BrdU immunoreactivity (green) localized to the nuclear compartment. Scale bars, 20 μm. ***B***, At 1 DIV, a proportion of cells show coexpression of nestin (green) and MAP2 (red), as evidenced by yellow fluorescence. The majority of cells are MAP2 positive. At 4 DIV, the majority of cells label positive for MAP2, whereas immunolabeling for nestin, GFAP, and MBP is rarely observed. These data are consistent with the previous demonstration that the majority (>99%) of cells, under these culture conditions, are phenotypically neuronal (Brewer et al., 1993; Brewer, 1995). Scale bars, 20 μm.

itor mixture (Sigma) for 30 min at 4°C. Cell lysates were centrifuged at 12,000 × *g* for 10 min, and the concentration of protein in the supernatant was determined by the BCA protein assay (Sigma). Twenty micrograms of total protein from whole-cell lysates were separated under reducing and denaturing conditions by 12% SDS-PAGE and electrotransferred to a polyvinylidene difluoride membrane (Millipore). Nonspecific binding sites were blocked with 5% skim milk in PBS containing 0.05% Tween 20 (PBS-Tween). A purified rabbit IgG recognizing the C-terminal domain of CDC2/p34 (ab7953; Novus Biologicals, Littleton, CO), a cell-proliferation marker (Gannon et al., 1998), was used to evaluate regulation of CDC2 expression. Mouse IgG2a (clone PC10; Zymed Laboratories, San Francisco, CA) directed to PCNA, a commonly used marker of cell proliferation (Gannon et al., 1998), was used to evaluate the cell proliferation. The membranes were incubated with CDC2 antibody (1:500 in PBS-Tween/1% goat serum) or PCNA antibody (1:1000 in PBS-Tween/1% horse serum) overnight at 4°C. Membranes were then incubated in horseradish peroxidase-conjugated goat anti-rabbit or horse anti-mouse IgG (1:6000), and results were visualized by the TMB Peroxidase Substrate kit (Vector Laboratories). Relative amounts of CDC2 and PCNA were quantified by optical density analysis using the UN-SCAN-IT gel automated digitizing system (Scion, Frederick, MD). The level was normalized with respect to GAPDH, a domestic loading control. Data are presented as means ± SEM for at least three independent experiments.

Statistical analyses. Differences in cell-proliferation markers were determined using one-way ANOVA, followed by a Neuman–Keuls *post hoc* analysis. Data derived from cDNA array or Western blot analyses represent semiquantitative estimates of the amount of a specific mRNA or protein that was present in a cell extract. The data displayed in graphs are reported as means ± SEM or fold change ± SEM of the actual scanning units derived from the densitometric analysis of each cDNA array or for Western blot densitometric units normalized to internal standard for protein content.

Results

Characterization of neuroprogenitor cells in primary cultures of embryonic day 18 rat hippocampal neurons

Dissociated cultures from E18 rat hippocampus were cultured in serum-free Neurobasal/B27 medium for 1–7 d. Immunochemical markers revealed that the cultures were predominantly neuronal in composition and also possessed a proportion of NPCs (Fig. 1*A*,*B*). Labeling for nestin, a large intermediate filament protein (class type VI) expressed during development and typically disappearing after E18, was used to identify progenitor cells (Fig. 1*A*, top) (Doetsch et al., 1997; Roy et al., 2000; Yamaguchi et al., 2000; Kawaguchi et al., 2001; Sawamoto et al., 2001; Romero-Ramos et al., 2002). Tuj1 labeling for neuron-specific βIII-microtubulin was conducted to identify cells committed to neuronal lineage (Fig. 1*A*, middle) (Menezes and Luskin, 1994; Menezes et al., 1995; Romero-Ramos et al., 2002). This antigen is not expressed by astrocytes or oligodendrocytes and is an early marker of neuronal differentiation for progenitor cells undergoing mitosis and for postmitotic neurons (Doetsch et al., 1997; Jacobs and Miller, 2000). Specific antibodies recognizing MAP2, a specific marker for postmitotic and differentiated neurons (Menezes and Luskin, 1994; Niijima et al., 1995; Young et al., 2000), GFAP, a specific marker for astrocytes, and MBP, a marker for oligodendrocytes, were also used. DAPI was used as a nuclear counterstain.

At 1 DIV, 27.4 ± 4.7% of cells were positive for nestin (Fig. 1*A*, top), 93 ± 6.3% of cells were positive for Tuj1 (Fig. 1*A*, middle), and 5.4% cells showed BrdU-positive nuclei (Fig. 1*A*, bottom), whereas at 7 DIV, no BrdU-positive nuclei were observed (data not shown). At 1 and 4 DIV, 96 ± 3.8 and 98 ± 1.6%, respectively, of the cells were positive for MAP2 (Fig. 1*B*). At 4 DIV, <2% of the cells were nestin positive, and <0.4% of the total cell population were GFAP and MBP positive. These results are consistent with previous reports indicating that neurons and their precursors make up the majority of postmitotic cultures and that glial cell contributions to the culture are reduced to <0.5% of the nearly pure neuronal population, as judged by immunocytochemistry for GFAP and neuron-specific enolase (Brewer et al., 1993; Brewer, 1995).

APα increases the number of nestin- and BrdU-positive cells

At 1 DIV, nestin-positive cells were found in clusters (as shown in Fig. 1*A*). In hippocampal cultures exposed to 500 nM APα, 36.3 ± 7.2% nestin-positive cells were observed compared with the 27.4 ± 4.7% observed in the control group, presenting a 32% increase in progenitor cells. This observation led us to perform a BrdU incorporation study to verify the proliferative effect of APα. Hippocampal neuron cultures were treated with either vehicle or 500 nM APα. Each set of cultures were exposed to BrdU (10 μM) for 4 h, followed by a 12 h of culture. Cultures treated with APα had a significantly greater number of BrdU-positive cells relative to vehicle control: 138 ± 10 (in every 2000 cells

counted) vs 108 ± 6 (in every 2000 cells) (see Fig. 3*B*), which represents a 26% increase in BrdU-positive cells relative to control (Fig. 2).

Biphasic dose–response of APα-induced BrdU incorporation

The dose–response of APα-induced proliferation was determined by chemiluminescence BrdU cell-proliferation ELISA. Data from three independent assays conducted in octuplets are presented in Figure 3. As a positive control, hippocampal neurons were treated with EGF (20 ng/ml), which induced a 40 ± 9% increase in BrdU incorporation. Exposure of hippocampal neurons to different concentrations of APα for 1 DIV showed a biphasic regulation in BrdU incorporation. Exposure of hippocampal neurons to different concentrations of APα for 1 DIV revealed a dose-dependent biphasic regulation of BrdU incorporation. At 100, 250, and 500 nM concentrations, APα significantly increased BrdU incorporation (lower concentrations were not statistically different from control). At 1000 nM, a reversal of the dose–response was first apparent, with higher doses shifting the response to significant repression of proliferation at 100–1000 μM. Comparison of neurogenic efficacy indicated that APα was nearly as efficacious as the growth factor EGF.

APα promotes the proliferation of neural progenitor cells derived from E18 rat hippocampus

To quantitatively assess the neurogenic efficacy of APα by FACS, primary cultures of rat hippocampal neurons were infected with MuLV–eGFP virus in the presence or absence of APα or APβ (serving as a negative control) 1 h after seeding for 4 h. The numbers of GFP-labeling dividing cells were measured by FACS at 2 DIV (Fig. 4*A*). In control cultures, 153 ± 12 per 2000 FACS sorted cells were positive for GFP. In cultures treated with 500 nM APα, 194 ± 17 per 2000 FACS sorted cells were positive (Table 1) and exhibited a 27% increase versus control (Fig. 4*B*). A slight but not statistically significant increase in GFP-positive cells was apparent in cultures treated with the stereoisomer APβ: 163 ± 11 per 2000 FACS sorted cells (Table 1, Fig. 4*B*). The 27% increase in the number of GFP-positive neurons induced by APα determined by FACS analysis is consistent with the percentage increase in BrdU incorporation (24 ± 9% for 250 nM and 28 ± 8% at 500 nM) and the total cell number determined by a nonfluorescent automatic cell counter, as shown in Figure 4*C*, in which a 28 ± 6 and 32 ± 12% increase in total cells was observed for 250 nM and 500 nM APα-treated groups, respectively, compared with the vehicle control group. These data are also consistent with the results derived from the nestin expression analyses, which showed a 32% increase in nestin-positive cells.

Under fluorescent microscopy, the morphology of GFP-

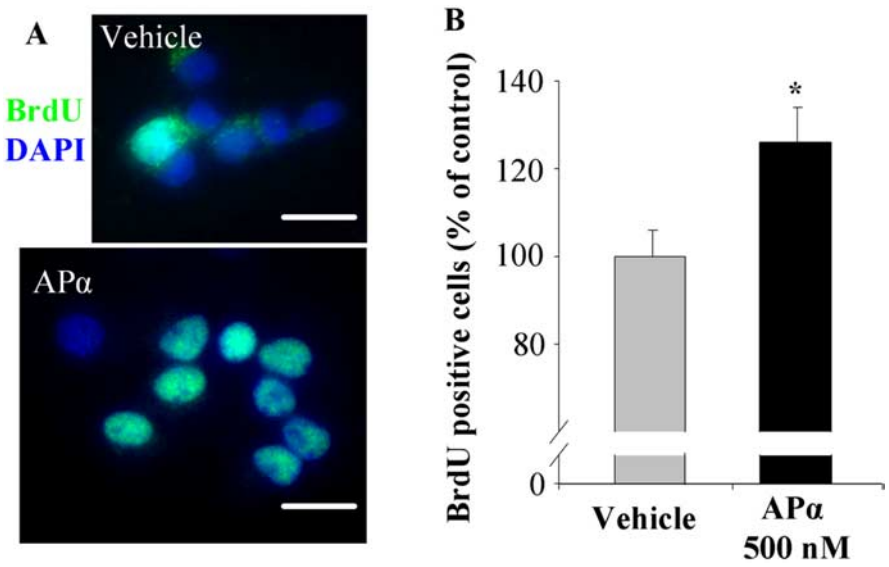

Figure 2. APα increases the nestin- and BrdU-positive cell numbers. ***A***, BrdU incorporation was visualized by specific BrdU antibody immunofluorescence. Photomicrographic images are representative of control (top) and 500 nM APα-treated (bottom) rat E18 hippocampal cultures after 1 DIV APα exposure. Scale bars, 20 μm. ***B***, Bar graph depicts quantitation of BrdU-positive cells from 10 randomly selected fields per slide. Total number of cells analyzed per slide was 800–1000. Three slides per condition were analyzed, for a total of 8964 cells contributing to the analysis. Data are from three independent experiments, and the results are plotted as mean ± SEM of BrdU-positive cells in percentage of vehicle group (set as 100%). *$p < 0.05$ versus vehicle.

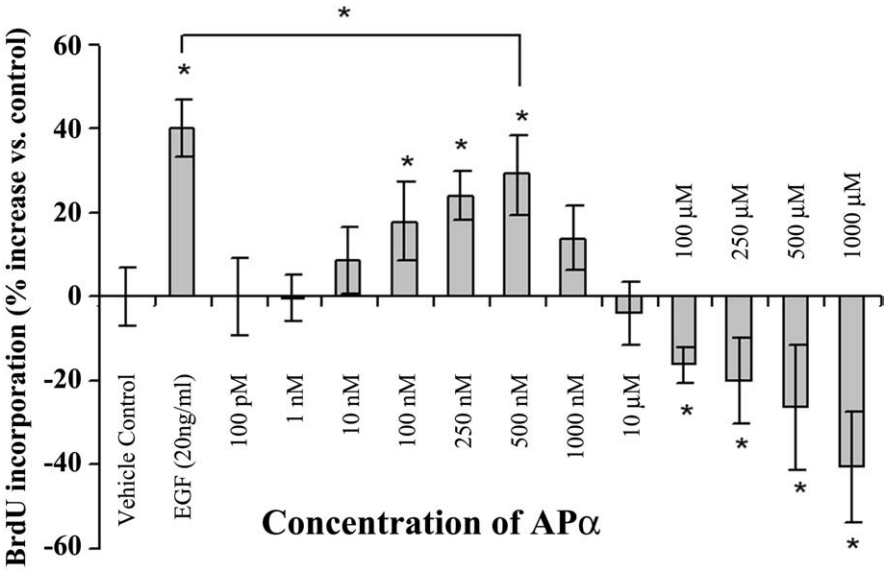

Figure 3. APα regulation of BrdU incorporation in rodent hippocampal neural progenitor cells is dose dependent. The dose–response of APα-induced proliferation was determined by chemiluminescence BrdU cell-proliferation ELISA. Exposure of hippocampal neurons to APα (100 pM to 1000 μM) for 24 h induced a biphasic regulation of BrdU incorporation. At 100–500 nM, APα significantly increased BrdU incorporation by 20 ± 11 to 30 ± 10%. At 1000 nM, a reversal of the dose–response was first apparent and shifted to repression of proliferation at >10 μM, with 1000 μM generating the greatest (40 ± 15%) repression. As a positive control, hippocampal neurons were treated with EGF (20 ng/ml), which induced a 40 ± 9% increase in BrdU incorporation. Data are from three independent assays conducted in octuplets. Results were plotted as percentage increase versus control (mean ± SEM). *$p < 0.05$ versus vehicle.

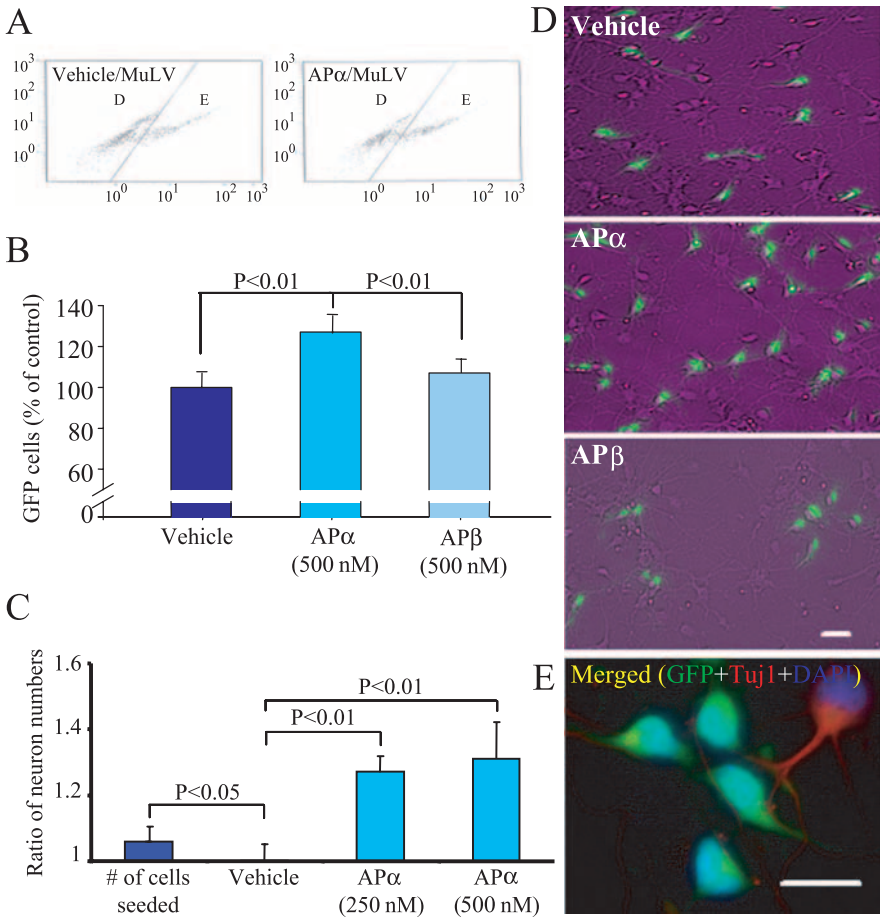

Figure 4. APα increases the proliferation of GFP-labeled hippocampal neural progenitor cells and the total number of cells. Cultures were treated with vehicle, 500 nM APα, or 500 APβ in the presence of MuLV–GFP retroviral particles (2×10^6/ml) for 4 h and further incubated with APα, APβ, or vehicle in the absence of MuLV–GFP retroviral particles for 44–48 h. ***A***, FACS profile. Area E presents the MuLV–GFP fluorescent cells, and area D presents the nonfluorescent cells. Results of FACS analysis indicated a greater number of cells sorted to the E fluorescent region. ***B***, The relative percentage of positive MuLV–GFP cells was plotted and shows that APα induced a 27% increase in the number of FACS sorted GFP-labeled neural progenitor cells, which was significantly increased above control and APβ conditions. The stereoisomer APβ was without effect on GFP incorporation into hippocampal neural progenitor cells. ***C***, Ratio of the total number of cells determined by particle size analyzer set to detect particles of 12–25 μm. Date derived from analysis of vehicle condition were set to 1, and data from other conditions are plotted relative to a vehicle value of 1. Analysis of total number of cells revealed that both 250 and 500 nM APα induced a significant increase in the number of cells. Data were derived from three independent experiments, analyzed by one-way ANOVA, followed by Neuman–Keuls *post hoc* analysis, and are presented as mean ± SEM. ***D***, Fluorescent microscopy images of MuLV–GFP-labeled cells. Each panel of ***D*** shows the fluorescent image overlaid onto the differential interference contrast image to visualize the underlying cells. Scale bar, 20 μm. ***E***, Coimmunolabeling of GFP-positive cells with the neuron-specific marker Tuj1 (red). Cells that coexpress GFP and Tuj1 appear yellow and label those cells that have divided and express a neuron-specific phenotype. Nuclei were counterstained with DAPI (blue). Scale bar, 20 μm.

Table 1. GFP-positive cell number per 2000 sorted cells

Experiments	Vehicle	APα	APβ
1	156 ± 12	201 ± 18	168 ± 9
2	147 ± 15	186 ± 19	170 ± 12
3	155 ± 11	194 ± 19	154 ± 7
Average	153 ± 12	194 ± 17*	163 ± 11

Summary of the number of MuLV–GFP-positive cells per 2000 hippocampal neurons sorted by FACS analysis after exposure to 500 nM APα, 500 nM APβ, or vehicle. *$p < 0.05$.

positive cells exhibited features of typical neurons, which were comparable with GFP-negative neurons (Fig. 4*D*), with a prominent nucleus and neurite extensions (Fig. 4*E*). GFP-positive cells also expressed positive Tuj1 immunoreactivity, indicating that these cells were of a neuronal lineage.

Validation of the MuLV–eGFP retrovirus as a strategy to determine neuron proliferation

To verify the accuracy of this strategy for neurogenesis determinations in primary hippocampal neurons, we executed FACS analyses in a constantly dividing hippocampal cell line, the mouse clonal HT-22 cell line, as a positive control. At 2 DIV after infection, 25–32% cells (449–638 per 2000 cells) were positive for GFP (Table 2), which is consistent with the one cell cycle per day mitotic rate for HT-22 cells (Sagara et al., 2002; Mize et al., 2003) and indicates that infection by MuLV–eGFP did not promote nor interfere with mitosis.

When HT-22 cells were treated with 500 nM APα, the number of GFP-positive cells increased to 680 ± 32 per 2000 FACS sorted cells, an increase of 22% over control condition (558 ± 28) for this continually dividing cell line at 2 DIV (Table 2, Fig. 5*A*). GFP-positive cells exhibited typical HT-22 cell morphology and GFP subcellular location (Fig. 5*B*). As a negative control, rat hippocampal neurons at 7 DIV treated with the same amount of viral loading showed no GFP-positive cells (data not shown), which is consistent with the BrdU incorporation results showing no BrdU incorporation in rat hippocampal cultures after 7 DIV.

Neurogenic effect of APα is stereospecific

To determine the steroid specificity for induction of neurogenesis, uptake of [^{3}H]thymidine incorporation was used as a surrogate marker of DNA synthesis and mitosis. Results (Fig. 6) of these analyses indicate that 250 nM APα induced a highly significant increase (150 ± 21%) in [^{3}H]thymidine incorporation relative to the control. Progesterone induced a 126 ± 12% increase ($p < 0.05$ vs control). Although the percentage average of progesterone was lower than that of APα, there was no statistical difference between them ($p > 0.05$) in [^{3}H]thymidine incorporation. However, the stereoisomers of APα, i.e., epiallopregnanolone and APβ, as well as 5α-pregnan-3β-ol were without effect. Additionally, allopregnandiol, 5α-pregnan-3α, 17α, 20α-triol, and pregnenolone sulfate, which we demonstrated to increase neurites number and length of primary cultured rat hippocampal neurons (our unpublished data), induced a significant decrease in [^{3}H]thymidine incorporation, which is consistent with their differentiation effect. The steroid specificity analysis provides evidence for both the specificity of APα-induced mitogenesis and supportive evidence that factors that promote morphological differentiation, such as pregnenolone sulfate, have an effect opposite to that of APα in primary cultured rat hippocampal progenitor cells.

Table 2. GFP-positive cell number per 2000 sorted cells

	GFP cells per 2000 sorted cells	
Experiments	Vehicle	APα
1	499 ± 28	609 ± 34
2	638 ± 32	783 ± 36
3	536 ± 24	648 ± 27
Average	558 ± 28	680 ± 32*

Summary of HT-22 cell FACS data indicating the number of MuLV–GFP-positive cells per 2000 sorted cells after exposure to 500 nM APα or vehicle. *$p < 0.05$.

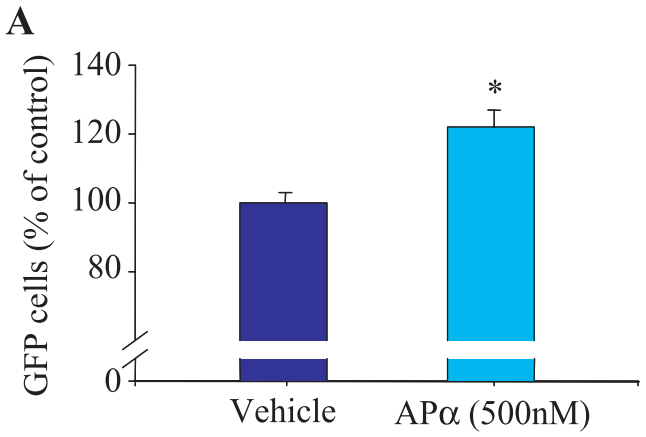

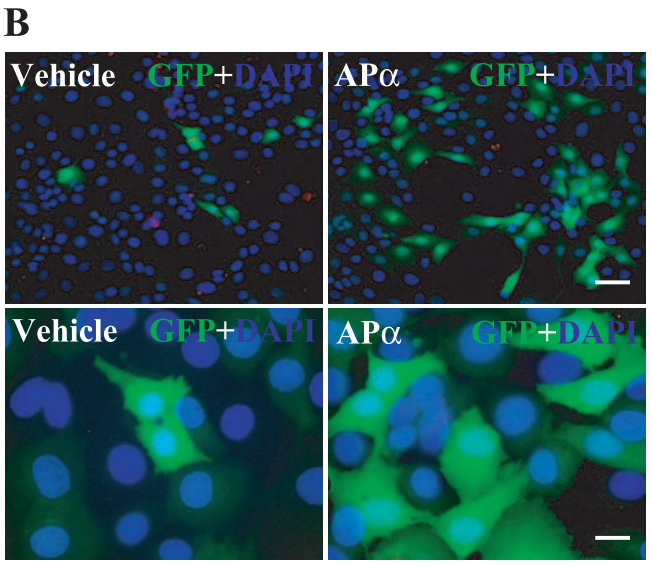

Figure 5. APα increased the number of MuLV–GFP-positive HT-22 cells. HT-22 cells were incubated with APα or vehicle in the presence of MuLV–GFP viral particles for 4 h and further incubated with APα or vehicle for another 44–48 h. The cells were either collected and sorted by FACS to analyze the number of GFP-positive cells or fixed to observe under fluorescent microscopy. ***A***, Bar graph depicts the percentage of GFP-positive cells in the APα group versus vehicle control (set as 100). *$p < 0.01$ versus control. ***B***, Fluorescent microscopic images showing morphology and relative density of GFP-positive cells in the APα-treated group versus control at low (top) and high (bottom) magnifications. Scale bars, 20 μm.

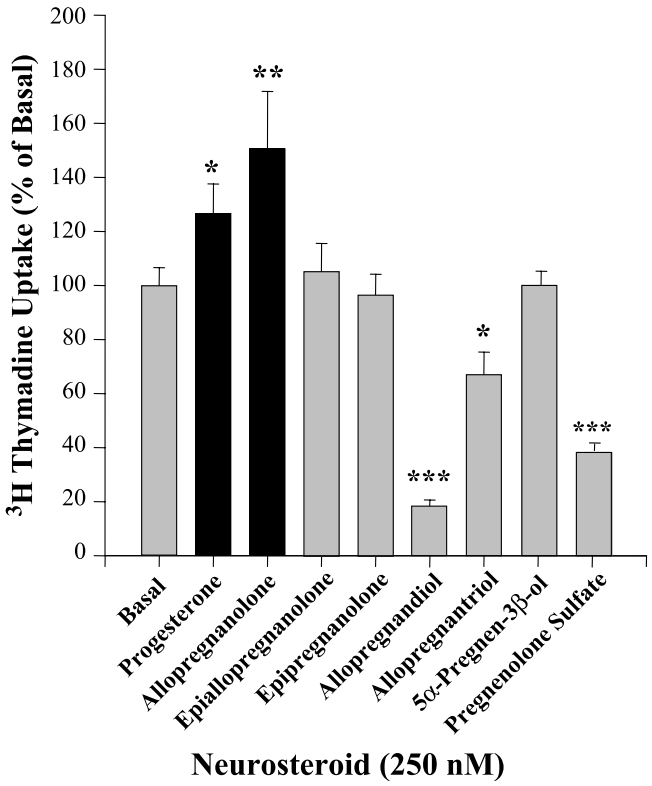

Figure 6. The neurogenic property of APα is specific and not shared by isomers or other steroids in the biosynthetic pathway. Rat hippocampal neurons were loaded with 1 μCi/ml [^{3}H]thymidine in the presence or absence of the indicated neurosteroids at 37°C for 24 h. APα induced a 150% increase in [^{3}H]thymidine incorporation relative to control. Moreover, DNA synthesis was specific to APα compared with other structurally and chemically similar steroids. P_4, the precursor molecule to APα, also induced a modest increase in [^{3}H]thymidine incorporation; however, the stereoisomers of allopregnanolone, epiallopregnanolone, and APβ, as well as 5α-pregnan-3β-ol, were without effect. Additionally, allopregnanediol, allopregnantriol, and pregnenolone sulfate induced a significant decrease in [^{3}H]thymidine incorporation. Data are expressed as mean ± SEM. *$p < 0.05$; **$p < 0.01$; ***$p < 0.001$.

APα treatment regulates gene expression for cell-cycle proteins

The mitogenic action of APα predicted the regulation of cell-cycle gene expression. To determine APα regulation of cell-cycle gene expression, we used a biased DNA gene array containing genes known to control cell proliferation. Primary cultures of rat hippocampal neurons were treated with 500 nM APα, which resulted in a marked upregulation of the genes that promotes the cell cycle, such as an eightfold increase in cyclin E, a protein that promotes progression from G_1 to S phase, a fourfold increase in two members of the M phase promoting factor complex, CDC2 (also called CDK1) and cyclin B, which promotes M phase transition required for completion of mitosis. In addition, another well defined cell-proliferation marker (Gannon et al., 1998; Graeber et al., 1998), PCNA, showed a more than twofold increase in expression. In contrast to the increase in cell-cycle genes involved in progression through the cell cycle, the expression of cell-cycle inhibitors CDK4 and CDK6, inhibitors p16 and p18, were decreased by more than twofold (Fig. 7*A*).

Because multiple endpoints were measured, there was an increased probability that differences in gene expression could occur by chance alone. To address this issue, the gene expression data were divided into subgroups of genes known to promote or inhibit cell proliferation, and the data from each subgroup of genes were subjected to multivariate ANOVA (Snedecor and Cochran, 1967; Jiang et al., 2002). Results of this analysis indicated a statistically significant effect of APα treatment on cyclins, CDKs, and CDK inhibitors (Table 3).

As validation of the gene-array data, real-time PCR was performed for five mRNAs coding for genes that promote transition through the cell cycle, two genes that inhibit cell-cycle progression, and two invariant genes. As presented in Figure 7*B*, 500 nM APα increased the mRNA expression: 9.61 ± 0.8-fold for cyclin E

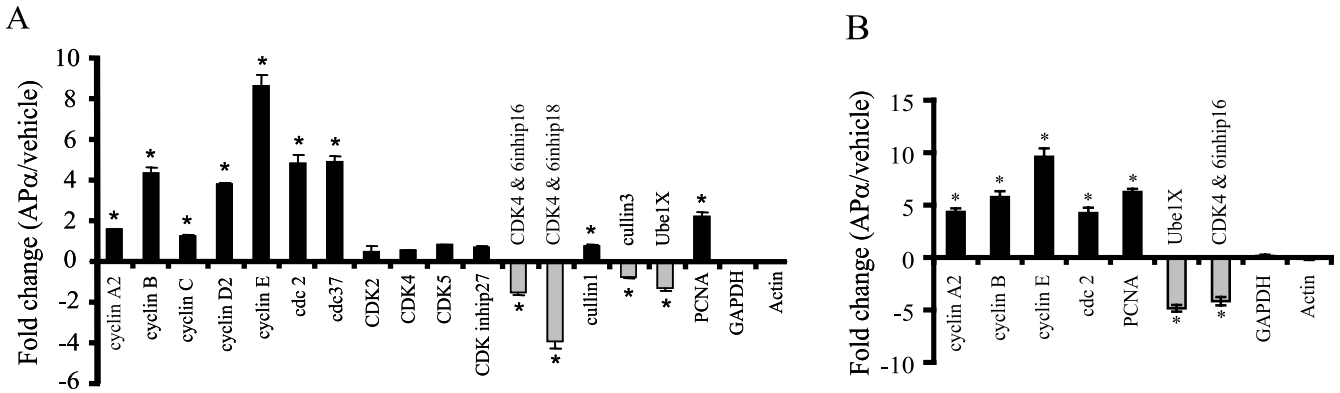

Figure 7. APα regulates cell-cycle gene expression. Cultures of hippocampal neurons were treated with vehicle or 500 nM APα for 24 h, followed by extraction of total RNA. ***A***, Gene array of cell-cycle-related gene expression. Nonradioactive probes were prepared and hybridized to a 96-gene miniarray. Two housekeeping genes (β-actin and GAPDH) were used as internal controls. Two blanks and pUC18 from bacterial plasmid were used as negative controls. Data were represented as fold change of mRNA expression in APα-treated neurons versus control (mean ± SEM) as determined by optical density. Results of these analyses in cultured hippocampal neurons indicate that APα induced a marked increase in genes that promote progression through the cell cycle while inhibiting genes associated with exiting the cell cycle. APα induced an eightfold increase in cyclin E, which promotes progression from G_1 to S phase, and a more than twofold increase in two well defined cell proliferation markers, CDC2 (also known as CDK1) and PCNA. In parallel to an increase in cell-cycle progression genes, APα inhibited the expression of CDK4 and CDK6 inhibitors and ubiquitin and cullin 3, which are associated with exiting the cell cycle. Two housekeeping genes, actin and GAPDH, were unchanged. Data were from three separate experiments, and multivariant ANOVA statistical analysis indicated that the increase and decrease were statistically significant, as presented in Table 3. ***B***, Validation of the gene-array results by real-time RT-PCR. APα induced a significant increase in mRNA expression of cyclin A2, cyclin B1, cyclin E, CDC2, and PCNA mRNA, whereas APα induced a significant reduction in mRNA for cyclin-dependent kinase inhibitor 2C (p18, inhibits CDK4) and ubiquitin-activating enzyme E1 (Ube1X). These quantitative PCR data are entirely consistent with the gene-array results. Data are depicted as fold change of mRNA expression in APα-treated neurons versus vehicle control (mean ± SEM) from three separate experiments. Controls were set to zero. *$p < 0.05$.

Table 3. Statistical summary of the effects of APα on cell-cycle gene expression using cDNA array analysis

Gene in categories	Multivariate statistic (APα vs control)	Univariate analysis (APα vs control)	Direction of change (APα vs control)
Cyclins	$p < 0.05$	Cyclin B, $p < 0.05$ Cyclin E2, $p < 0.05$	Increased
CDKs	$p < 0.05$	Cdc2 (CDK1), $p < 0.05$	Increased
CDK inhibitors	$p < 0.05$	CDK int 16, $p < 0.05$	Decreased
Ubiquitin relatives	$p < 0.05$	Cullin 3, $p < 0.05$ Ube1X, $p < 0.05$ Cullin 1, $p < 0.05$	Decreased
PCNA	$p < 0.05$	PCNA, $p < 0.05$	Increased
Actin and GAPDH	$p < 0.5$	GAPDH, $p < 0.5$	No change

Cultures of hippocampal neurons were treated with vehicle or 500 nM APα for 24 h, followed by extraction of total RNA. Nonradioactive probes were prepared and hybridized to gene array. Data were determined by optical density and subjected to multivariate ANOVA. Ube1X, Ubiquitin-activating enzyme E1. CDK int 16, CDK inhibitor P16.

versus control; 5.76 ± 0.56 for cyclin B; 4.24 ± 0.51 for CDC2; and 6.35 ± 0.3 for PCNA. In addition, cyclin A2, an S phase expression protein, increased 4.35 ± 0.34-fold. In contrast, APα treatment decreased the mRNA expression of Cdkn2c (p18) 4.84 ± 0.32-fold and ubiquitin-activating enzyme E1 4.16 ± 0.4-fold versus control. These results are entirely consistent with the direction of change indicated by the gene-array data, although the real-time PCR data indicate a slightly greater magnitude of fold change. Together, these data indicate that APα promotes the expression of activators of cell-cycle progression, such as cyclins, CDKs, and PCNA, while simultaneously downregulating the CDK inhibitors and other ubiquitin-related genes.

APα increases the protein level of cell-proliferating markers CDC2 and PCNA

Based on the results of the gene-array analysis, two well defined cell-proliferating markers, CDC2 and PNCA, were further analyzed by Western blot to determine whether increases in mRNA for mitotic cell-cycle genes were indicative of increases in protein. Whole-cell lysates from hippocampal neurons treated with 500 nM APα and control neurons were assessed by Western blot for CDC2 and PNCA. As shown in Figure 8, *A* and *B*, both CDC2 and PNCA protein levels were elevated by 1.5- or 2-fold by APα. These results indicate that APα significantly increased protein expression for two cell-cycle proteins, CDC2 and PCNA, which are required for progression through mitosis. These data are consistent with the mRNA increases observed in the cell-cycle gene expression analysis.

Antagonist to VGLCC abolishes APα-induced neuronal cell proliferation

Based on previous findings from our group that demonstrated that APα induced a significant rise in intracellular calcium in cultured hippocampal neurons during 1–10 d *in vitro* that was dependent on the $GABA_AR$ and the VGLCC (Son et al., 2002), we determined whether the neurogenic effect of APα was antagonized by the VGLCC blocker nifedipine. Nifedipine alone had no effect on rat hippocampal primary culture proliferation, whereas nifedipine completely abolished 500 nM APα-induced NPC proliferation increase (Fig. 9). These results indicate that APα requires activation of the VGLCC to promote neurogenesis.

APα induces proliferation of human neural stem cells from the cerebral cortex

To determine whether our findings in rat neural progenitor cells were relevant to proliferation of human neural stem cells, we investigated the neurogenic properties of APα in human neural stem cells derived from the human cerebral cortex (Jakel et al., 2004; Suzuki et al., 2004). Results of those analyses indicate that APα induced a highly significant increase in BrdU incorporation (35 ± 10 to 49 ± 15% increase vs control in the range of 1–500 nM APα). As with the rNPCs, APα-induced neurogenesis in the hNSCs was dose dependent and exhibited a biphasic response. APα was a more potent neurogenic factor in the hNSCs with a minimally effective dose of 1 nM, whereas in the rNPCs the min-

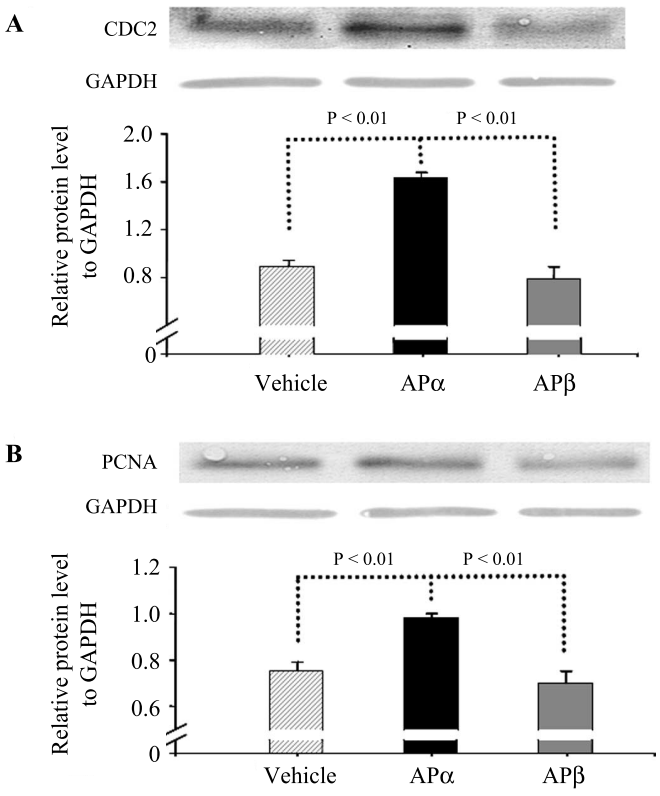

Figure 8. APα increases protein expression of CDC2 and PCNA. Rat hippocampal neurons in primary culture were treated with vehicle, APα (500 nM), or APβ (500 nM) for 24 h and processed for Western blots. Results of Western blot analysis indicate that APα induced a significant increase in the protein level for CDC2 (***A***) and PCNA (***B***). The increase in protein level was specific to APα, because the stereoisomer APβ was without effect. Bar graphs represent mean ± SEM, and data were analyzed by one-way ANOVA, followed by Neuman–Keuls *post hoc* analysis.

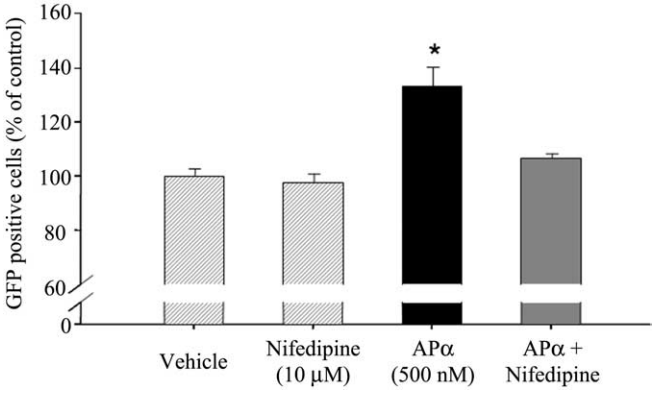

Figure 9. APα-induced proliferation of neural progenitor cells requires activation of the L-type calcium channel. MuLV–GFP viral particle-infected rat hippocampal neurons were treated with vehicle, nifedipine (an L-type calcium channel antagonist), APα, or APα plus nifedipine. Nifidipine (10 μM) completely abolished the proliferative effect of APα, which was detected by FACS analysis of GFP-positive cells. Data are from three independent experiments and presented as percentage of GFP-positive cells in each group versus control (set as 100%). *$p < 0.01$ versus control, nifedipine, or APα plus nifedipine.

imally effective dose was 100 nM. The efficacy of APα as a neurogenic factor in hNSCs was comparable with that induced by bFGF (20 ng/ml) plus heparin (5 μg/ml) treatment (30 ± 9% increase vs control) (Fig. 10*A*). The stem cell marker nestin (Fig. 10*B*) and the neural progenitor marker Tuj1 (Fig. 10*C*) were both expressed in the human neural stem cells.

Discussion

In this study, we demonstrated that APα specifically increased proliferation of rat hippocampal NPCs and human cerebral cortical NSCs in a dose-dependent manner. In parallel, APα significantly increased expression of genes that promote progression through the cell cycle while inhibiting expression of genes involved in cell-cycle repression. Immunocytochemical labeling for NPC markers indicated that the newly formed cells are of neuronal lineage. Furthermore, we determined that the mechanism for APα-induced neurogenesis requires activation of VGLCCs.

Potency and efficacy of APα-induced neurogenesis

APα-induced neurogenesis was a dose-dependent process, with concentrations within the 10^{-9} to mid 10^{-7} M range promoting proliferation, whereas concentrations in excess of 10^{-6} M significantly inhibiting neurogenesis. The biphasic effect of APα on neurogenesis is supported by a recent study showing that nanomolar levels of APα increase whereas micromolar levels of APα inhibit the proliferation of polysialylated form of the neural cell adhesion molecule (PSA-NCAM)-positive neural progenitors (Gago et al., 2004). At high concentrations (i.e., in micromolar), APα can be converted by 20α hydroxysteroid dehydrogenase to allopregnanediol (Wiebe and Lewis, 2003) and hence may increase the local concentration of allopregnanediol that inhibited DNA replication of rNPC, thereby inducing a biphasic dose–response.

APα was a more potent neurogenic factor for hNSCs with a minimally effective dose of 1 nM, whereas in the rNPCs the minimally effective dose was >10 nM. The concentrations of APα required to induce neurogenesis *in vitro* are comparable with those found in both rat and human brain. APα levels are 12 ng/g (~38 nM) in the pregnant maternal rat brain and 19 ng/g (~60 nM) within the embryonic rat brain (Concas et al., 1998; Grobin and Morrow, 2001). In the human premenopausal female, APα levels in serum are 4 nM in the middle of menstrual cycle (Wang et al., 1996; Genazzani et al., 1998) and are 160 nM during the third trimester in healthy pregnant women (Luisi et al., 2000). Because a similar concentration has been detected in the umbilical cord, it is suggested to be an indicator of fetal levels of APα (Luisi et al., 2000).

In contrast to fetal development, an age-associated decrease in serum APα was observed in men >40 yr of age but remarkably not in women (Genazzani et al., 1998). Interestingly, a significant decrease (approximately threefold) in APα levels was observed in patients with Alzheimer's disease compared with the age-matched control group (Bernardi et al., 2000; Weill-Engerer et al., 2002). In parallel, in the aged brain, both the pool of NSC and their proliferative potential are markedly diminished (Jin et al., 2003; Wise, 2003; Enwere et al., 2004).

Reported herein, APα-induced neurogenesis ranged from 20 to 30% in the rodent NPCs to 37–49% in the human neural stem cells. The efficacy of APα as a neurogenic factor is comparable with that induced by bFGF plus heparin from our own study and also in agreement with previously published results. For example, bFGF induced a 0.4-fold increase in cultured rat brain-derived progenitor cells (Gago et al., 2003) after 3 d treatment and a 25% increase in BrdU incorporation in 3-month-old rat brain (Jin et al., 2003). Additional support comes from the recent studies that APα induces an ~20% increase in thymidine incorporation in immatured rat cerebral granular cells (Keller et al., 2004) and a

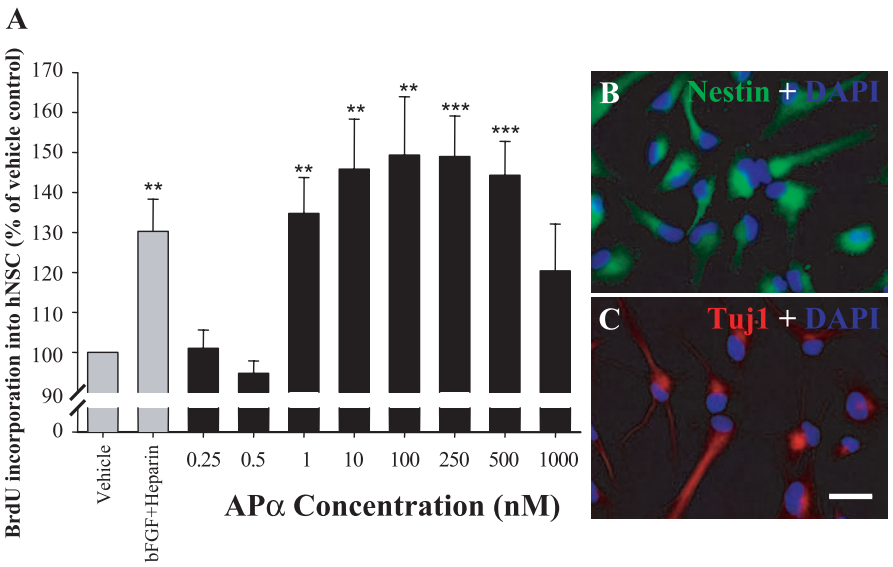

Figure 10. APα increases BrdU incorporation in human neural stem cells from the cerebral cortex in a dose-dependent manner. ***A***, BrdU incorporation in human cerebral cortical stem cells was measured by a chemiluminescence BrdU ELISA. APα induced a dose-dependent biphasic increase in BrdU incorporation. The minimally effective concentration was 1 nM APα (38 ± 10% increase), with the maximal proliferative effect achieved at 10–500 nM APα (43 ± 14 to 49 ± 15% increase). At 1000 nM, a reversal of the increase in BrdU incorporation was apparent. The positive control, bFGF (20 ng/ml) plus heparin (5 μM/ml) induced a 30 ± 9% increase in BrdU incorporation versus control. Data were derived from at least three independent assays conducted in octuplets. Results were plotted as percentage of vehicle control (mean ± SEM). $^{**}p < 0.01$ versus vehicle; $^{***}p < 0.001$ versus control. ***B*** shows a representative cluster of nestin-positive neural stem cells, and ***C*** shows Tuj1-positive human neural stem cells. Cell nuclei were counterstained with DAPI. Scale bar, 15 μm.

20–30% increase in PSA-NCAM-positive progenitor proliferation derived from rat brain (Gago et al., 2004). Together, these data indicate that APα can promote neurogenesis of neural stem cells derived from multiple sites within the rodent brain and from the cerebral cortex of human brain.

Genetic and proliferative properties of APα-induced neurogenesis

The gene-array and real-time RT-PCR data are consistent with a neurogenic effect of APα. Genes that promote transition through the cell cycle and proliferation, such as cyclins and CDKs, including CDC2, cyclin B, and PNCA, were upregulated by APα. Correspondingly, APα downregulated the expression of genes involved in inhibition and degradation of CDKs and cyclins, such as CDK4 and CDK6 inhibitor p16, p18, cullin 3, and ubiquitin-activating enzyme E1, enzymes that are required for ubiquitination of mitotic cyclins and promote exit from the cell cycle (Schulman et al., 2000; Tyers and Jorgensen, 2000). In our study, APα not only regulated the expression of cell-cycle proteins and DNA amplification but also drove a complete mitosis of the rNPCs. This conclusion is supported by the data showing that APα increases the MuLV–GFP-positive cell number, because GFP signal can only be observed in the cells that transversed a complete cell cycle (Roe et al., 1993; Lewis and Emerman, 1994; Bieniasz et al., 1995). Moreover, the APα-induced increase in total cell number further supports this conclusion.

Mechanism of APα-induced neurogenesis

It is well known that APα acts as an allosteric modulator of the $GABA_AR$ to increase chloride influx, thereby hyperpolarizing the neuronal membrane potential and decreasing neuron excitability (Gee et al., 1987, 1988, 1995). In marked contrast to this action in mature neurons, activation of $GABA_AR$ by GABA or APα in immature neurons, leads to an efflux of chloride. The high intracellular chloride content in embryonic cells reverses the concentration gradient for chloride, whereby the efflux of chloride leads to depolarization of the membrane and opening of VGLCCs (Berninger et al., 1995; Dayanithi and Tapia-Arancibia, 1996; Son et al., 2002; Perrot-Sinal et al., 2003). Blockade of APα-induced neurogenesis by an inhibitor of VGLCCs is consistent with our finding of an APα-induced rise in intracellular calcium via activation of VGLCCs (Son et al., 2002).

Increases in intracellular calcium can activate calcium-dependent mechanisms of mitosis in early precursor cells and human NSCs to promote neurogenesis (Owens and Kriegstein, 1998; Owens et al., 2000; Ashworth and Bolsover, 2002). We demonstrated that APα induces a rapid and developmentally regulated influx of calcium via $GABA_AR$ activation of VGLCCs (Son et al., 2002) in cultured hippocampal neurons, which may evoke neurogenesis. Thus, we propose that the $GABA_AR$-activated VGLCCs and subsequent calcium influx plays a key role in the APα-stimulated neurogenesis in both rat neural progenitors and human neural stem cells.

Source of APα in brain

The synthesis of the neurosteroids, progesterone, and its metabolite APα in brain, first identified by Baulieu, is now well established (Baulieu, 1997; Baulieu et al., 2001; Mellon and Griffin, 2002a,b). A region-specific expression pattern of progesterone-converting enzymes, P450scc, 5α reductase, and 3α hydroxysteroid dehydrogenase, in brain is evident in both hippocampus and cortex. (Baulieu and Robel, 1990; Mellon and Griffin, 2002a,b; Stoffel-Wagner et al., 2003). Remarkably, the enzymes 5α-reductase and 3α-hydroxysteroid dehydrogenase, required to convert progesterone to its 3α metabolites, are present and functional in pluripotential progenitors (Lauber and Lichtensteiger, 1996; Melcangi et al., 1996). In the peripheral nervous system and CNS, both APα and progesterone can promote oligodendrocyte proliferation and myelination (Gago et al., 2001, 2004; Schumacher et al., 2004).

The present study demonstrated that both progesterone and APα promotes DNA amplification in rNPCs. Thus, the presence of progesterone in B27, a supplement of the medium, very likely contributes to proliferation. However, statistical analyses of APα effects were compared with control, which also contained progesterone. Thus, the APα-induced results are superimposed on that induced in the presence of progesterone. Furthermore, it is not clear whether progesterone-induced proliferation is a direct or an indirect process accomplished by its metabolite, APα. In the CNS, APα and its precursor progesterone are primarily produced from 5α-pregnane-3,20-dione by 3α-hydroxysteroid oxidoreductase in astrocytes (Krieger and Scott, 1989; Zwain and Yen, 1999). In addition, Micevych et al. (2003) demonstrated that

estrogen increased the synthesis of progesterone in astrocytes. The relationship between astrocyte synthesis of neurogenic neurosteroids, APα and progesterone, and the ability of astrocytes to promote neurogenesis (Song et al., 2002) remains to be determined.

Therapeutic potential of APα to promote neurogenesis

Unlike large molecular weight growth factors, such as FGF and neurotrophins, which do not readily pass the blood–brain barrier and induce untoward side effects in humans (Lie et al., 2004), APα, with a steroidal chemical structure and low molecular weight of 318.49, easily penetrates the blood–brain barrier to induce CNS effects, including anxiolytic and sedative hypnotic properties (Gee et al., 1988; Brinton, 1994). Results of developing APα as an antiepileptic/antianxiety therapeutic studies indicated no toxicology issues in healthy human volunteers (Monaghan et al., 1997) and therapeutic benefit without adverse events in children with refractory infantile spasms (Kerrigan et al., 2000). Together with our present data, these findings suggest a promising strategy for promoting neurogenesis in the aged brain and potentially for restoration of neuronal populations in brains recovering from neurodegenerative disease or injury. Studies are currently underway to determine the neurogenic potential of APα in rodent models of aging and Alzheimer's disease.

References

Ashworth R, Bolsover SR (2002) Spontaneous activity-independent intracellular calcium signals in the developing spinal cord of the zebrafish embryo. Brain Res Dev Brain Res 139:131–137.

Baulieu EE (1997) Neurosteroids: of the nervous system, by the nervous system, for the nervous system. Recent Prog Horm Res 52:1–32.

Baulieu EE, Robel P (1990) Neurosteroids: a new brain function? J Steroid Biochem Mol Biol 37:395–403.

Baulieu EE, Schumacher M (2000) Progesterone as a neuroactive neurosteroid, with special reference to the effect of progesterone on myelination. Hum Reprod 15:1–13.

Baulieu EE, Robel P, Schumacher M (2001) Neurosteroids: beginning of the story. Int Rev Neurobiol 46:1–32.

Ben-Ari Y, Khalilov I, Represa A, Gozlan H (2004) Interneurons set the tune of developing networks. Trends Neurosci 27:422–427.

Bernardi F, Salvestroni C, Casarosa E, Nappi RE, Lanzone A, Luisi S, Purdy RH, Petraglia F, Genazzani AR (1998) Aging is associated with changes in allopregnanolone concentrations in brain, endocrine glands and serum in male rats. Eur J Endocrinol 138:316–321.

Bernardi F, Lanzone A, Cento RM, Spada RS, Pezzani I, Genazzani AD, Luisi S, Luisi M, Petraglia F, Genazzani AR (2000) Allopregnanolone and dehydroepiandrosterone response to corticotropin-releasing factor in patients suffering from Alzheimer's disease and vascular dementia. Eur J Endocrinol 142:466–471.

Berninger B, Marty S, Zafra F, da Penha Berzaghi M, Thoenen H, Lindholm D (1995) GABAergic stimulation switches from enhancing to repressing BDNF expression in rat hippocampal neurons during maturation in vitro. Development 121:2327–2335.

Bieniasz PD, Weiss RA, McClure MO (1995) Cell cycle dependence of foamy retrovirus infection. J Virol 69:7295–7299.

Brewer GJ (1995) Serum-free B27/neurobasal medium supports differentiated growth of neurons from the striatum, substantia nigra, septum, cerebral cortex, cerebellum, and dentate gyrus. J Neurosci Res 42:674–683.

Brewer GJ, Torricelli JR, Evege EK, Price PJ (1993) Optimized survival of hippocampal neurons in B27-supplemented Neurobasal, a new serum-free medium combination. J Neurosci Res 35:567–576.

Brinton RD (1994) The neurosteroid 3 α-hydroxy-5 α-pregnan-20-one induces cytoarchitectural regression in cultured fetal hippocampal neurons. J Neurosci 14:2763–2774.

Cherubini E, Rovira C, Gaiarsa JL, Corradetti R, Ben Ari Y (1990) GABA mediated excitation in immature rat CA3 hippocampal neurons. Int J Dev Neurosci 8:481–490.

Ciriza I, Azcoitia I, Garcia-Segura LM (2004) Reduced progesterone metabolites protect rat hippocampal neurones from kainic acid excitotoxicity in vivo. J Neuroendocrinol 16:58–63.

Concas A, Mostallino MC, Porcu P, Follesa P, Barbaccia ML, Trabucchi M, Purdy RH, Grisenti P, Biggio G (1998) Role of brain allopregnanolone in the plasticity of gamma-aminobutyric acid type A receptor in rat brain during pregnancy and after delivery. Proc Natl Acad Sci USA 95:13284–13289.

Dayanithi G, Tapia-Arancibia L (1996) Rise in intracellular calcium via a nongenomic effect of allopregnanolone in fetal rat hypothalamic neurons. J Neurosci 16:130–136.

Deisseroth K, Singla S, Toda H, Monje M, Palmer TD, Malenka RC (2004) Excitation-neurogenesis coupling in adult neural stem/progenitor cells. Neuron 42:535–552.

Doetsch F, Garcia-Verdugo JM, Alvarez-Buylla A (1997) Cellular composition and three-dimensional organization of the subventricular germinal zone in the adult mammalian brain. J Neurosci 17:5046–5061.

Enwere E, Shingo T, Gregg C, Fujikawa H, Ohta S, Weiss S (2004) Aging results in reduced epidermal growth factor receptor signaling, diminished olfactory neurogenesis, and deficits in fine olfactory discrimination. J Neurosci 24:8354–8365.

Gago N, Akwa Y, Sananes N, Guennoun R, Baulieu EE, El Etr M, Schumacher M (2001) Progesterone and the oligodendroglial lineage: stage-dependent biosynthesis and metabolism. Glia 36:295–308.

Gago N, Avellana-Adalid V, Evercooren AB, Schumacher M (2003) Control of cell survival and proliferation of postnatal PSA-NCAM(+) progenitors. Mol Cell Neurosci 22:162–178.

Gago N, El-Etr M, Sananes N, Cadepond F, Samuel D, Avellana-Adalid V, Baron-Van Evercooren A, Schumacher M (2004) 3alpha,5alpha-Tetrahydroprogesterone (allopregnanolone) and gamma-aminobutyric acid: autocrine/paracrine interactions in the control of neonatal PSA-NCAM+ progenitor proliferation. J Neurosci Res 78:770–783.

Gannon JV, Nebreda A, Goodger NM, Morgan PR, Hunt T (1998) A measure of the mitotic index: studies of the abundance and half-life of p34cdc2 in cultured cells and normal and neoplastic tissues. Genes Cells 3:17–27.

Gee KW, Chang WC, Brinton RE, McEwen BS (1987) GABA-dependent modulation of the Cl^- ionophore by steroids in rat brain. Eur J Pharmacol 136:419–423.

Gee KW, Bolger MB, Brinton RE, Coirini H, McEwen BS (1988) Steroid modulation of the chloride ionophore in rat brain: structure-activity requirements, regional dependence and mechanism of action. J Pharmacol Exp Ther 246:803–812.

Gee KW, Lan NC, Bolger MB, Wieland S, Belelli D, Chen JS (1992) Pharmacology of a $GABA_A$ receptor coupled steroid recognition site. Adv Biochem Psychopharmacol 47:111–117.

Gee KW, McCauley LD, Lan NC (1995) A putative receptor for neurosteroids on the $GABA_A$ receptor complex: the pharmacological properties and therapeutic potential of epalons. Crit Rev Neurobiol 9:207–227.

Genazzani AR, Petraglia F, Bernardi F, Casarosa E, Salvestroni C, Tonetti A, Nappi RE, Luisi S, Palumbo M, Purdy RH, Luisi M (1998) Circulating levels of allopregnanolone in humans: gender, age, and endocrine influences. J Clin Endocrinol Metab 83:2099–2103.

Graeber MB, Lopez-Redondo F, Ikoma E, Ishikawa M, Imai Y, Nakajima K, Kreutzberg GW, Kohsaka S (1998) The microglia/macrophage response in the neonatal rat facial nucleus following axotomy. Brain Res 813:241–253.

Griffin LD, Gong W, Verot L, Mellon SH (2004) Niemann-Pick type C disease involves disrupted neurosteroidogenesis and responds to allopregnanolone. Nat Med 10:704–711.

Grobin AC, Morrow AL (2001) 3Alpha-hydroxy-5alpha-pregnan-20-one levels and $GABA_A$ receptor-mediated $36Cl^-$ flux across development in rat cerebral cortex. Brain Res Dev Brain Res 131:31–39.

Jacobs JS, Miller MW (2000) Cell cycle kinetics and immunohistochemical characterization of dissociated fetal neocortical cultures: evidence that differentiated neurons have mitotic capacity. Brain Res Dev Brain Res 122:67–80.

Jakel RJ, Schneider BL, Svendsen CN (2004) Using human neural stem cells to model neurological disease. Nat Rev Genet 5:136–144.

Jiang W, Zhu Z, Bhatia N, Agarwal R, Thompson HJ (2002) Mechanisms of energy restriction: effects of corticosterone on cell growth, cell cycle machinery, and apoptosis. Cancer Res 62:5280–5287.

Jin K, Sun Y, Xie L, Batteur S, Mao XO, Smelick C, Logvinova A, Greenberg

DA (2003) Neurogenesis and aging: FGF-2 and HB-EGF restore neurogenesis in hippocampus and subventricular zone of aged mice. Aging Cell 2:175–183.

Kawaguchi A, Miyata T, Sawamoto K, Takashita N, Murayama A, Akamatsu W, Ogawa M, Okabe M, Tano Y, Goldman SA, Okano H (2001) Nestin-EGFP transgenic mice: visualization of the self-renewal and multipotency of CNS stem cells. Mol Cell Neurosci 17:259–273.

Keller EA, Zamparini A, Borodinsky LN, Gravielle MC, Fiszman ML (2004) Role of allopregnanolone on cerebellar granule cells neurogenesis. Brain Res Dev Brain Res 153:13–17.

Kerrigan JF, Shields WD, Nelson TY, Bluestone DL, Dodson WE, Bourgeois BF, Pellock JM, Morton LD, Monaghan EP (2000) Ganaxolone for treating intractable infantile spasms: a multicenter, open-label, add-on trial. Epilepsy Res 42:133–139.

Krieger NR, Scott RG (1989) Nonneuronal localization for steroid converting enzyme: 3 alpha-hydroxysteroid oxidoreductase in olfactory tubercle of rat brain. J Neurochem 52:1866–1870.

Lauber ME, Lichtensteiger W (1996) Ontogeny of 5 alpha-reductase (type 1) messenger ribonucleic acid expression in rat brain: early presence in germinal zones. Endocrinology 137:2718–2730.

Lewis PF, Emerman M (1994) Passage through mitosis is required for oncoretroviruses but not for the human immunodeficiency virus. J Virol 68:510–516.

Lie DC, Song H, Colamarino SA, Ming GL, Gage FH (2004) Neurogenesis in the adult brain: new strategies for central nervous system diseases. Annu Rev Pharmacol Toxicol 44:399–421.

Liu QY, Chang YH, Schaffner AE, Smith SV, Barker JL (2002) Allopregnanolone activates $GABA_A$ receptor/Cl^- channels in a multiphasic manner in embryonic rat hippocampal neurons. J Neurophysiol 88:1147–1158.

Luisi S, Petraglia F, Benedetto C, Nappi RE, Bernardi F, Fadalti M, Reis FM, Luisi M, Genazzani AR (2000) Serum allopregnanolone levels in pregnant women: changes during pregnancy, at delivery, and in hypertensive patients. J Clin Endocrinol Metab 85:2429–2433.

MacKrell AJ, Soong NW, Curtis CM, Anderson WF (1996) Identification of a subdomain in the Moloney murine leukemia virus envelope protein involved in receptor binding. J Virol 70:1768–1774.

Melcangi RC, Froelichsthal P, Martini L, Vescovi AL (1996) Steroid metabolizing enzymes in pluripotential progenitor central nervous system cells: effect of differentiation and maturation. Neuroscience 72:467–475.

Melcangi RC, Magnaghi V, Martini L (1999) Steroid metabolism and effects in central and peripheral glial cells. J Neurobiol 40:471–483.

Mellon SH, Griffin LD (2002a) Synthesis, regulation, and function of neurosteroids. Endocr Res 28:463.

Mellon SH, Griffin LD (2002b) Neurosteroids: biochemistry and clinical significance. Trends Endocrinol Metab 13:35–43.

Menezes JR, Luskin MB (1994) Expression of neuron-specific tubulin defines a novel population in the proliferative layers of the developing telencephalon. J Neurosci 14:5399–5416.

Menezes JR, Smith CM, Nelson KC, Luskin MB (1995) The division of neuronal progenitor cells during migration in the neonatal mammalian forebrain. Mol Cell Neurosci 6:496–508.

Micevych P, Sinchak K, Mills RH, Tao L, LaPolt P, Lu JK (2003) The luteinizing hormone surge is preceded by an estrogen-induced increase of hypothalamic progesterone in ovariectomized and adrenalectomized rats. Neuroendocrinology 78:29–35.

Mize AL, Shapiro RA, Dorsa DM (2003) Estrogen receptor-mediated neuroprotection from oxidative stress requires activation of the mitogen-activated protein kinase pathway. Endocrinology 144:306–312.

Monaghan EP, Navalta LA, Shum L, Ashbrook DW, Lee DA (1997) Initial human experience with ganaxolone, a neuroactive steroid with antiepileptic activity. Epilepsia 38:1026–1031.

Niijima K, Chalmers GR, Peterson DA, Fisher LJ, Patterson PH, Gage FH (1995) Enhanced survival and neuronal differentiation of adrenal chromaffin cells cografted into the striatum with NGF-producing fibroblasts. J Neurosci 15:1180–1194.

Nilsen J, Brinton RD (2003) Divergent impact of progesterone and medroxyprogesterone acetate (Provera) on nuclear mitogen-activated protein kinase signaling. Proc Natl Acad Sci USA 100:10506–10511.

Owens DF, Kriegstein AR (1998) Patterns of intracellular calcium fluctuation in precursor cells of the neocortical ventricular zone. J Neurosci 18:5374–5388.

Owens DF, Flint AC, Dammerman RS, Kriegstein AR (2000) Calcium dynamics of neocortical ventricular zone cells. Dev Neurosci 22:25–33.

Palmer TD, Takahashi J, Gage FH (1997) The adult rat hippocampus contains primordial neural stem cells. Mol Cell Neurosci 8:389–404.

Perrot-Sinal TS, Auger AP, McCarthy MM (2003) Excitatory actions of GABA in developing brain are mediated by l-type Ca^{2+} channels and dependent on age, sex, and brain region. Neuroscience 116:995–1003.

Pomata PE, Colman-Lerner AA, Baranao JL, Fiszman ML (2000) In vivo evidences of early neurosteroid synthesis in the developing rat central nervous system and placenta. Brain Res Dev Brain Res 120:83–86.

Roe T, Reynolds TC, Yu G, Brown PO (1993) Integration of murine leukemia virus DNA depends on mitosis. EMBO J 12:2099–2108.

Romero-Ramos M, Vourc'h P, Young HE, Lucas PA, Wu Y, Chivatakarn O, Zaman R, Dunkelman N, el-Kalay MA, Chesselet MF (2002) Neuronal differentiation of stem cells isolated from adult muscle. J Neurosci Res 69:894–907.

Roy NS, Wang S, Jiang L, Kang J, Benraiss A, Harrison-Restelli C, Fraser RA, Couldwell WT, Kawaguchi A, Okano H, Nedergaard M, Goldman SA (2000) In vitro neurogenesis by progenitor cells isolated from the adult human hippocampus. Nat Med 6:271–277.

Sagara Y, Ishige K, Tsai C, Maher P (2002) Tyrphostins protect neuronal cells from oxidative stress. J Biol Chem 277:36204–36215.

Sawamoto K, Nakao N, Kakishita K, Ogawa Y, Toyama Y, Yamamoto A, Yamaguchi M, Mori K, Goldman SA, Itakura T, Okano H (2001) Generation of dopaminergic neurons in the adult brain from mesencephalic precursor cells labeled with a nestin-GFP transgene. J Neurosci 21:3895–3903.

Schulman BA, Carrano AC, Jeffrey PD, Bowen Z, Kinnucan ER, Finnin MS, Elledge SJ, Harper JW, Pagano M, Pavletich NP (2000) Insights into SCF ubiquitin ligases from the structure of the Skp1-Skp2 complex. Nature 408:381–386.

Schumacher M, Weill-Engerer S, Liere P, Robert F, Franklin RJ, Garcia-Segura LM, Lambert JJ, Mayo W, Melcangi RC, Parducz A, Suter U, Carelli C, Baulieu EE, Akwa Y (2003) Steroid hormones and neurosteroids in normal and pathological aging of the nervous system. Prog Neurobiol 71:3–29.

Schumacher M, Guennoun R, Robert F, Carelli C, Gago N, Ghoumari A, Gonzalez Deniselle MC, Gonzalez SL, Ibanez C, Labombarda F, Coirini H, Baulieu EE, De Nicola AF (2004) Local synthesis and dual actions of progesterone in the nervous system: neuroprotection and myelination. Growth Horm IGF Res 14 [Suppl A]:S18–S33.

Snedecor GW, Cochran WG (1967) Statistical methods, Ed 6, pp 258–296. Ames, IA: Iowa State UP.

Son M, Dietrich A, Brinton RD (2002) Allopregnanolone induces a rapid transient rise in intracellular calcium in embryonic hippocampal neurons. Soc Neurosci Abstr 28:272.8.

Soneoka Y, Cannon PM, Ramsdale EE, Griffiths JC, Romano G, Kingsman SM, Kingsman AJ (1995) A transient three-plasmid expression system for the production of high titer retroviral vectors. Nucleic Acids Res 23:628–633.

Song H, Stevens CF, Gage FH (2002) Astroglia induce neurogenesis from adult neural stem cells. Nature 417:39–44.

Stoffel-Wagner B, Watzka M, Steckelbroeck S, Ludwig M, Clusmann H, Bidlingmaier F, Casarosa E, Luisi S, Elger CE, Beyenburg S (2003) Allopregnanolone serum levels and expression of 5 alpha-reductase and 3 alpha-hydroxysteroid dehydrogenase isoforms in hippocampal and temporal cortex of patients with epilepsy. Epilepsy Res 54:11–19.

Suzuki M, Wright LS, Marwah P, Lardy HA, Svendsen CN (2004) Mitotic and neurogenic effects of dehydroepiandrosterone (DHEA) on human neural stem cell cultures derived from the fetal cortex. Proc Natl Acad Sci USA 101:3202–3207.

Tyers M, Jorgensen P (2000) Proteolysis and the cell cycle: with this RING I do thee destroy. Curr Opin Genet Dev 10:54–64.

van den Pol AN (2004) Developing neurons make the switch. Nat Neurosci 7:7–8.

van Praag H, Schinder AF, Christie BR, Toni N, Palmer TD, Gage FH (2002) Functional neurogenesis in the adult hippocampus. Nature 415:1030–1034.

Wachs FP, Couillard-Despres S, Engelhardt M, Wilhelm D, Ploetz S, Vroemen M, Kaesbauer J, Uyanik G, Klucken J, Karl C, Tebbing J, Svendsen C, Weidner N, Kuhn HG, Winkler J, Aigner L (2003) High efficacy of

clonal growth and expansion of adult neural stem cells. Lab Invest 83:949–962.

Wang M, Seippel L, Purdy RH, Backstrom T (1996) Relationship between symptom severity and steroid variation in women with premenstrual syndrome: study on serum pregnenolone, pregnenolone sulfate, 5 alpha-pregnane-3,20-dione and 3 alpha-hydroxy-5 alpha-pregnan-20-one. J Clin Endocrinol Metab 81:1076–1082.

Weill-Engerer S, David JP, Sazdovitch V, Liere P, Eychenne B, Pianos A, Schumacher M, Delacourte A, Baulieu EE, Akwa Y (2002) Neurosteroid quantification in human brain regions: comparison between Alzheimer's and nondemented patients. J Clin Endocrinol Metab 87:5138–5143.

Wiebe JP, Lewis MJ (2003) Activity and expression of progesterone metabolizing 5alpha-reductase, 20alpha-hydroxysteroid oxidoreductase and 3alpha(beta)-hydroxysteroid oxidoreductases in tumorigenic (MCF-7, MDA-MB-231, T-47D) and nontumorigenic (MCF-10A) human breast cancer cells. BMC Cancer 3:9.

Wise PM (2003) Creating new neurons in old brains. Sci Aging Knowledge Environ 2003:PE13.

Yamaguchi M, Saito H, Suzuki M, Mori K (2000) Visualization of neurogenesis in the central nervous system using nestin promoter-GFP transgenic mice. NeuroReport 11:1991–1996.

Young MJ, Ray J, Whiteley SJ, Klassen H, Gage FH (2000) Neuronal differentiation and morphological integration of hippocampal progenitor cells transplanted to the retina of immature and mature dystrophic rats. Mol Cell Neurosci 16:197–205.

Zwain IH, Yen SS (1999) Neurosteroidogenesis in astrocytes, oligodendrocytes, and neurons of cerebral cortex of rat brain. Endocrinology 140:3843–3852.